Analysis of Neuronal Source Dynamics and Connectivity During Seizure

Tim Mullen[1,2*], Zeynep Akalin Acar[1], Jason Palmer[1], Gregory Worrell[3], Scott Makeig[1]

[1] Swartz Center for Computational Neuroscience//INC, [2] Dept. of Cognitive Science, UC, San Diego, [3] Dept. of Neurology, Mayo Clinic

* tim@sccn.ucsd.edu

Abstract

Understanding the dynamics of neural processes critically involved in initiating and propagating a seizure may help in devising novel methods of seizure detection, intervention and treatment. Furthermore, applications of novel dynamical analysis methods in clinical situations where there is some "ground truth" can validate methods for more general application to cognitive neuroscience. In this poster we analyze neuronal dynamics during epileptic seizures using adaptive multivariate autoregressive (VAR) models applied to quasi-independent (ICA) sources of intracranial EEG (iEEG, ECoG) data recorded from subdural electrodes implanted in a human patient for presurgery monitoring. We analyze the time-frequency dynamics of directed information flow between sources using a multivariate granger-causal method, identifying distinct information flow motifs in different stages of the seizure. We then further examine the spatial distribution in the cortical source domain of causal sources and sinks of ictal activity using a novel combination of graph theoretic metrics and Sparse Bayesian Learning source localization. Finally, we apply an eigendecomposition method to decompose the VAR model into a system of decoupled oscillators and relaxators (eigenmodes) with characteristic damping times and frequencies. We demonstrate that analysis of a small subset of the most dynamically important eigenmodes may allow effective detection of ictal onset and offset, while also yielding insight into the dynamical structure of the neuronal system. Convergent evidence from these analyses reveals distinct stages in the seizure which correspond to shifts in the spatiotemporal dynamics and connectivity structure between sources in or near the clinically-identified epileptic foci.

Seizure ECoG Data

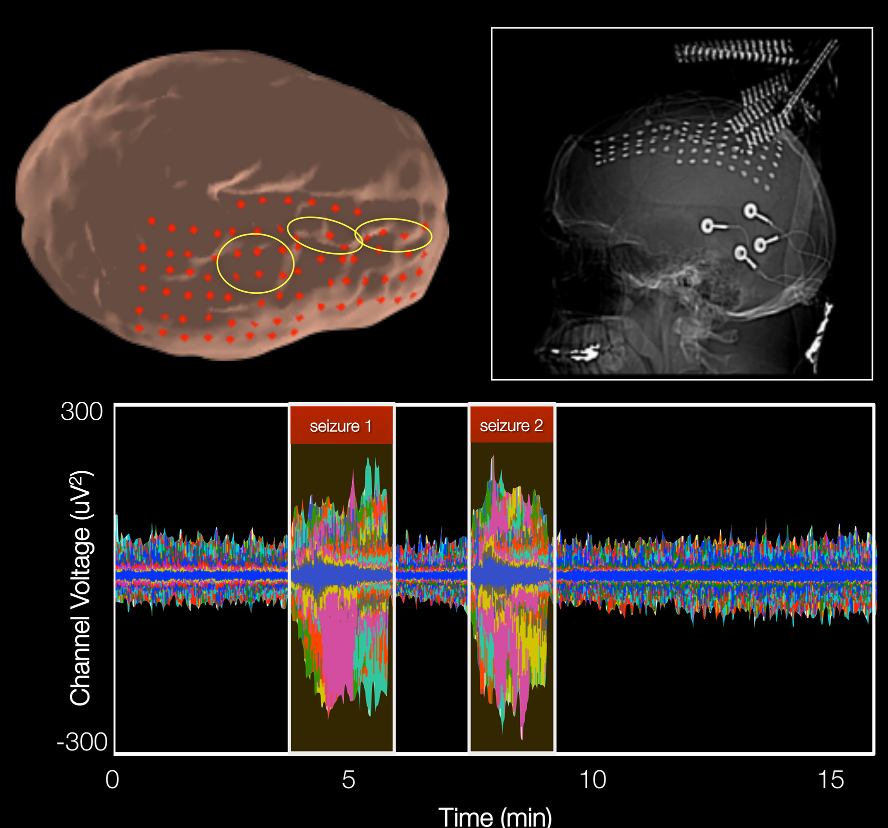

- Intracranial EEG (ECoG) from one patient undergoing pre-surgical evaluation for treatment of partial refractory epilepsy due to porencephalic cyst in right frontoparietal brain
- 78 subdural ECoG electrodes (1 mm diameter, 10 mm spacing), 29 scalp
- 16 minutes ECoG resting data, 500 Hz
- 2 seizures (1.9 min & 1.5 min
- Provided by Dr. Greg Worrell, Mayo Clinic

Theory: Channel or Source?

$$X(t) = MS(t) = \sum_{k=1}^{p} MA^{(k)}(t)M^{-1}X(t-k) + ME(t)$$

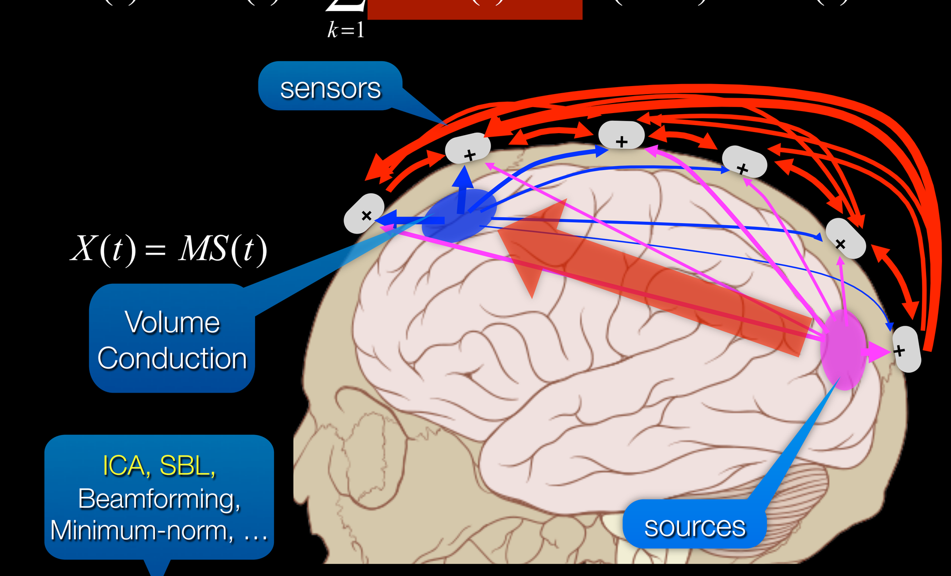

$$X(t) = MS(t)$$

$$S(t) = \sum_{k=1}^{p} A^{(k)}(t)S(t-k) + E(t)$$

Volume conduction exists for ECoG too!
(c.f. Whitmer, Worrell, ..., Makeig, *Frontiers in Neuro.* 2010)

Analyzing connectivity on the level of the electrode suffers from spatial ambiguity and a high risk of false positives due to volume conduction. If sources are convolutional (e.g. VAR), rather than identifying spatiotemporal mixing matrices $A^{(\cdot)}$ – which describe source connectivity – we instead identify $MA^{(\cdot)}M^{-1}$ – a transformation of this matrix, at all lags, by the forward mixing matrix. This can lead to spurious connectivity estimates. One solution is to identify M^{-1} and $S(t)$ (source reconstruction) and thus identify $A^{(\cdot)}$.

Method Pipeline

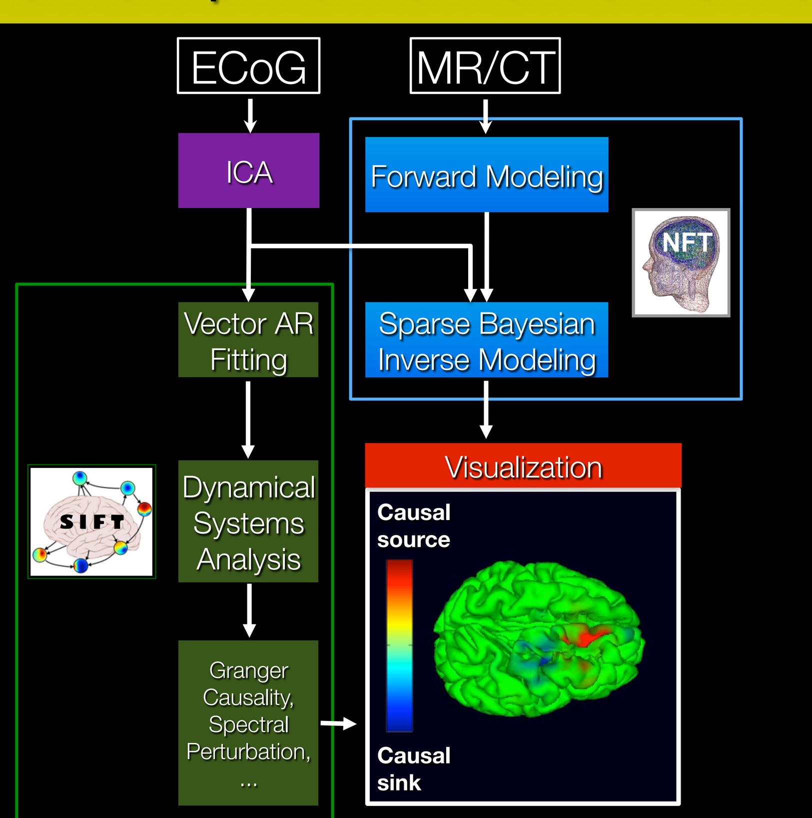

Independent Component Analysis

Infomax ICA separates channel data **X(t)** into maximally instantaneously independent latent sources **S(t)** under the linear model **X(t)=*M*S(t)**. Independent components (ICs) corresponding to artifacts can be rejected [1]. Remaining ICs – which generally have improved SNR relative to channel data – can be localized and examined for remaining time-delayed dependencies. An additional benefit of ICA is that is provides dimensionality reduction making single-trial time-varying dynamical systems analysis tractable. ICA was applied to the ECoG data and seizure activity separated into a subspace of 16 ICs which we retained for further analysis.

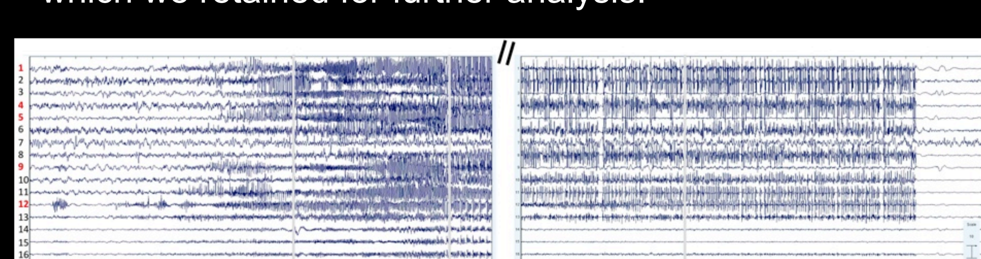

Forward Model and Multiscale Sparse Bayesian Inverse Model

Accurate source localization requires anatomically-realistic forward models and appropriately constrained inverse models [2-3]. We construct a Boundary Element Method (BEM) forward model from the patient's CT/MR images modeling cortex, grid, scalp, and skull.

We model each IC source as arising from a sparse, distributed collection of overlapping multi-scale gaussian-shaped patches of cortical tissue. This produces a 240K-element patch dictionary (3 patches centered at each of 80K cortical mesh vertices). We find the sum of the smallest number of patches (a sparse multiscale basis) which best explains a given observed ICA component map.

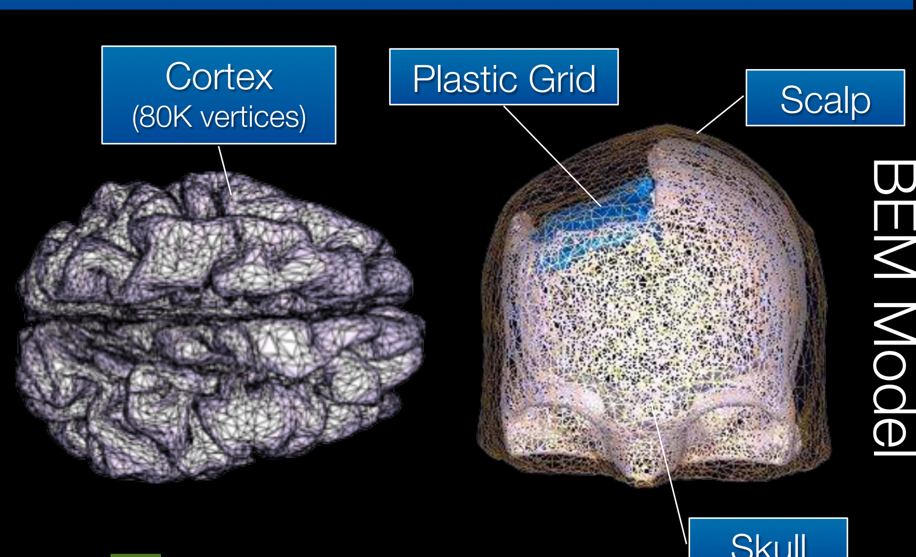

Legend			
symb	number of...	symb	number of...
m	channels (78)	c	ICs (16)
v	source voxels (80K)	T	time points (120K)

$$W_{ij}^{(k)} = gauss(D_{ij},\sigma_k) = \frac{1}{\sqrt{2\pi\sigma_k^2}} exp\left(-\frac{D_{ij}^2}{2\sigma_k^2}\right)$$

$$\sigma_k = scale/3$$

Three truncated Gaussian patches of different scales

radius	10 mm	6 mm	3 mm
σ_k	3.33 mm	2 mm	1 mm

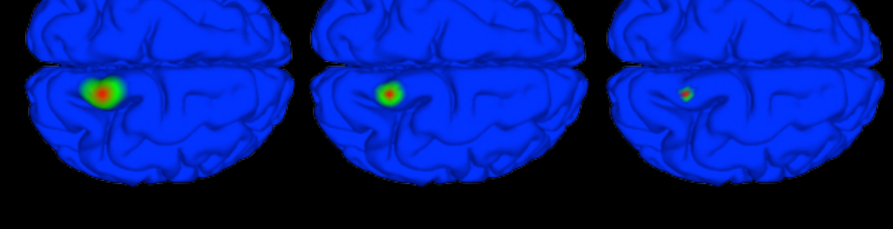

Forward Model

$$X = LS$$

$$L := [m \times v] \quad \text{Lead Field Matrix}$$

$$\tilde{L} = [LW^{(1)} \cdots LW^{(3)}]_{m\times 3v}$$

ICA Model

$$X = A\hat{S}$$

$$\hat{S}_q := [1 \times T] \quad q^{th} \text{ IC activation}$$

ICA+SBL Inverse Model

$$A_q = \tilde{L}\tilde{M}_q + \epsilon_q$$

$$\tilde{L}^{-1} = \mathrm{SBL}(A_q, \tilde{L})$$

$$\tilde{M}_q = [\tilde{L}^{-1}A_q]_{3v\times 1}$$

$$M_q = reshape(\tilde{M}_q, v \times 3)$$

$$M_q = \sum_{i=1}^{3} M_{q(:,i)}$$

$$P_q = M_q\hat{S}_q \quad [v \times T] \text{ cortical surface potentials for } q^{th} \text{ IC}$$

Dynamical Systems Analysis and Multivariate Granger Causality

VAR[p] model (with frequency transform)

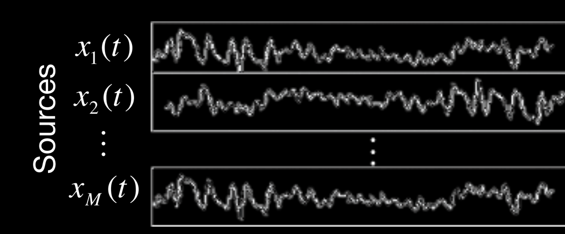

$$\mathbf{X}(t) = \sum_{k=1}^{p} \mathbf{A}^{(k)}(t)\mathbf{X}(t-k) + \mathbf{E}(t)$$

$$\mathbf{A}(f,t) = -\sum_{k=0}^{p} \mathbf{A}^{(k)}(t)e^{-i2\pi fk}; \quad \mathbf{A}^{(0)} = I$$

$$\mathbf{X}(f,t) = \mathbf{A}(f,t)^{-1}\mathbf{E}(f,t) = \mathbf{H}(f,t)\mathbf{E}(f,t)$$

Multivariate Granger Causality

Spectrum

$$S(f,t) = \mathbf{X}(f,t)\mathbf{X}(f,t)^* = \mathbf{H}(f,t)\Sigma\mathbf{H}(f,t)^*$$

Partial Coherence

$$P_{ij}(f,t) = \frac{S_{ij}^{-1}(f,t)}{\sqrt{S_{ii}^{-1}(f,t)S_{jj}^{-1}(f,t)}}$$

(Brillinger, 1996; Dahlhaus, 2000)

Full-frequency Directed Transfer Function

$$\eta_{ij}^2(f,t) = \frac{|H_{ij}(f,t)|^2}{\sum_f \sum_{k=1}^{M} |H_{ik}(f,t)|^2}$$

(Kaminski, 1991; Korzeniewska, 2003)

Direct DTF

$$\delta_{ij}^2(f,t) = \eta_{ij}^2(f,t)P_{ij}^2(f,t)$$

(Korzeniewska, 2003, 2010)

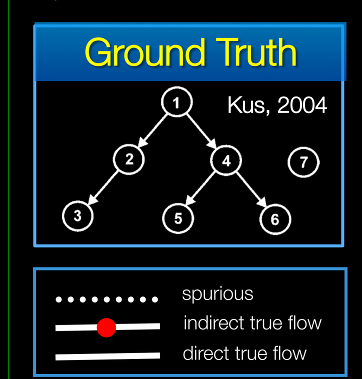

A locally-stationary dynamical system can be modeled as an adaptive vector autoregressive (VAR[p]) model of order *p*. A VAR[7] model was fit to the 16-dim seizure IC subspace (down-sampled to 256 Hz) in 15-sec sliding windows. Whiteness tests (Portmanteau) and stability analysis were carried out. Conditional (multivariate) Granger-causality (dDTF [4]) was estimated and significance of information flow determined by phase-randomization.

We utilize several graph-theoretic metrics to help simplify complex network structure and identify cortical areas that act as granger-causal "hubs" or drivers (e.g. epileptogenic foci) – which we denote a causal "source" as opposed to a "sink"

Graph Theoretic Measures

C : Asymmetric (e.g. causal) connectivity matrix

- Outflow $O_j = \sum_{i=1}^{M} C_{ij}$
- Inflow $I_i = \sum_{j=1}^{M} C_{ij}$
- Causal Flow $F_i = O_i - I_i$
- Asymmetry Ratio $R_i = \frac{O_i - I_i}{O_i + I_i}$

Multi-lag Eigenmode Analysis of Principal Oscillation Patterns

Any stable *M*-dim VAR[p] process can be decomposed into *Mp*, *M*-dim decoupled eigenmodes, each of which can be characterized as a stochastically-forced damped oscillator or relaxator with a characteristic frequency and damping time [5]. The damping time provides a measure of how long, on average, an oscillation is seen before noise an unobserved or nonlinear dynamical processes become increasingly important. The most *dynamically important* eigenmodes provide a measure of the ***principal oscillation pattern*** of the system.

Visualization

We developed a novel method that visualized univariate graph-theoretic metrics associated with specific IC sources (e.g. causal flow, outflow, etc) directly on the cortical surface by projecting these metrics through the SBL solution. This affords an intuitive spatiotemporal visualization of cortical network dynamics.

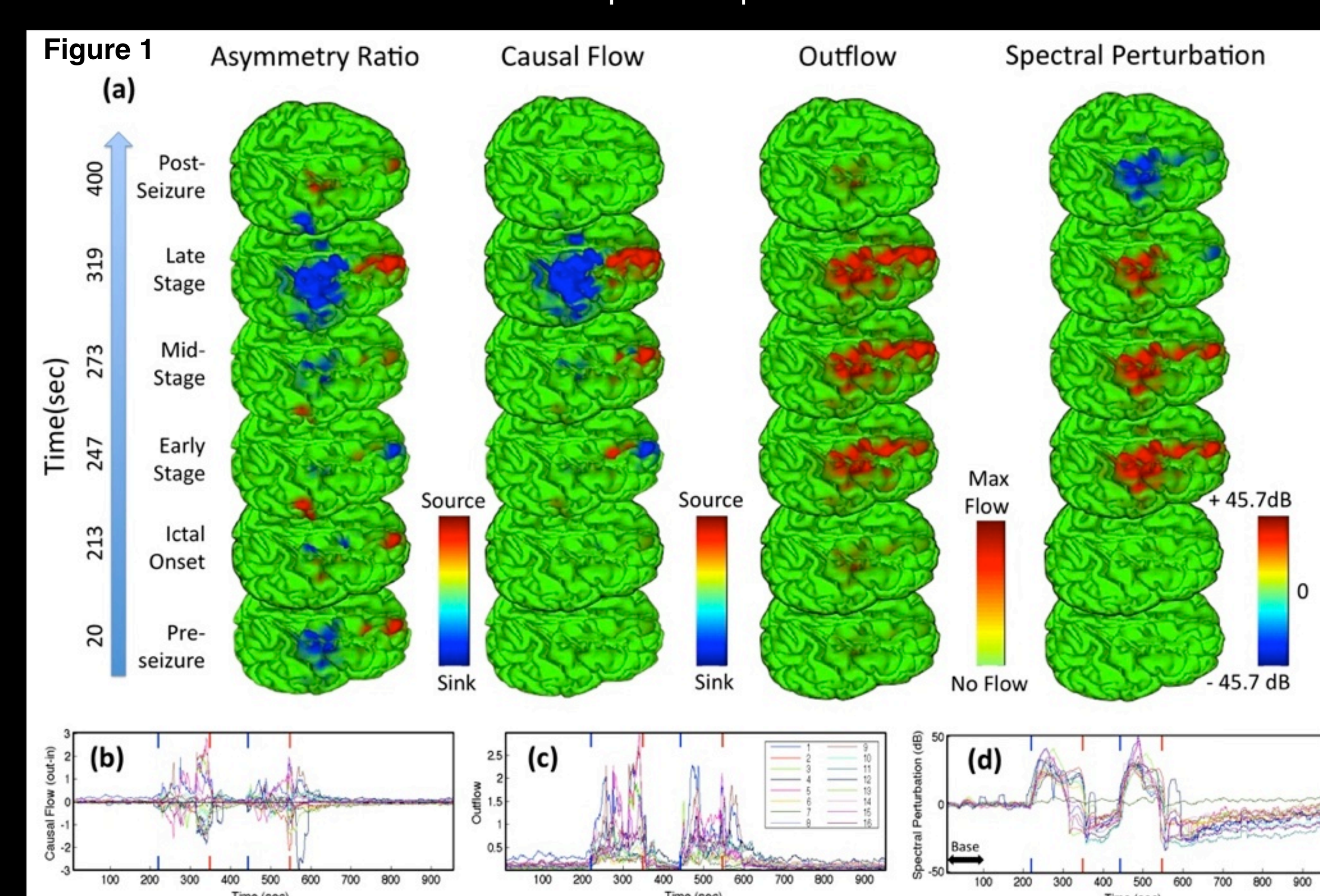

Figure 1: Panel (a) shows a sequence of frames from animations mapping 4-30 Hz causal and spectral measures projected onto the cortical surface before, after and during different stages of the first seizure. Colormaps bounded at 99th percentile. Panels (b-d) show, respectively, the causal flow, outflow, and spectral perturbation (deviation from 1-100 second baseline power indicated by horizontal doublearrow) for all IC sources as a function of time. Blue (Red) vertical ticks denote onset (offset) of both seizures.

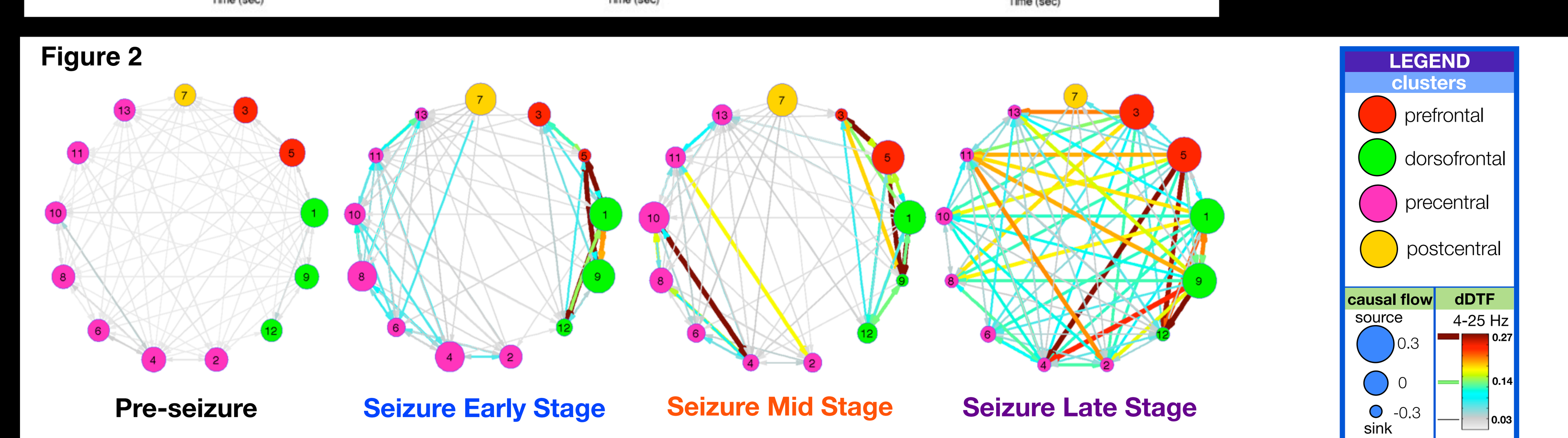

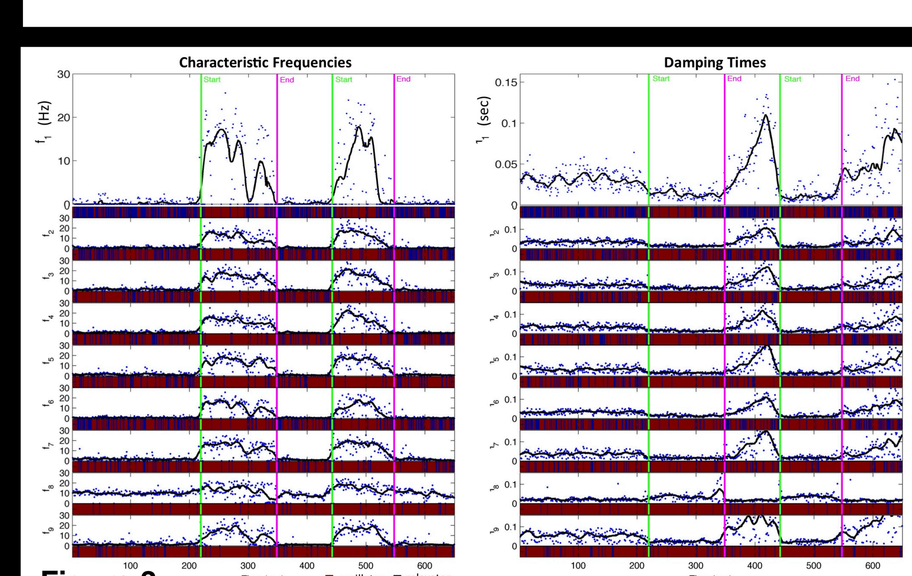

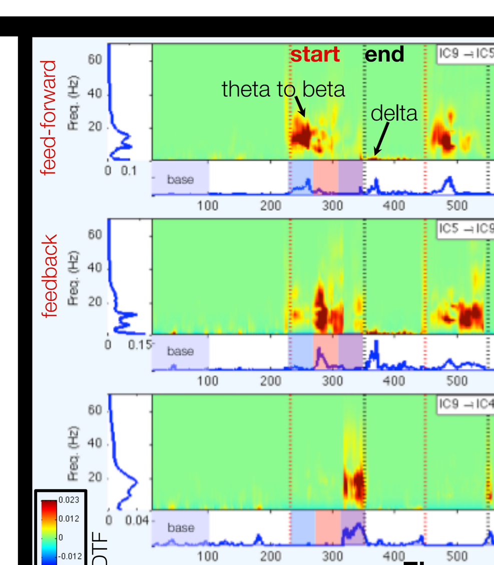

Fig. 2: Radial plots showing network motifs for 13 most dynamically important ICs in different stages of the first seizure (2nd seizure is very similar). ***Fig. 3:*** Characteristic frequencies (left) and damping times (right) for the 8% most dynamically important eigenmodes, in descending order of importance. Green (Magenta) vertical lines denote onset (offset) of seizure. ***Fig. 4:*** Representative time-frequency images showing causal influence between select ICs during multiple seizure stages.

Conclusions

Our novel spatiotemporal analysis allowed us to localize causal source and sink hubs emerging during seizure. We observed distinct stages of principal oscillation pattern shift and alternating information flow between adjacent or overlapping frontal gyri and sulci which may be maintained through short U-fiber connections. In a final seizure stage this was followed by a strong asymmetric spread of activity from frontal to parietal networks, possibly maintained by cortico-cortical tracts or subcortical U-fibers. Extensions of this approach may have clinical applications as well as applications in basic cognitive neuroscience research.

References and Acknowledgements

Support: San Diego Fellowship (TM), Glushko Fellowhsip (TM), ONR, NIMH, NINDS, and The Swartz Foundation (Old Field, NY)

References: [1] Makeig, S., Bell., A., et al, (1996) *NIPS* [2] R. Ramirez, S. Makeig. (2007) HBM. [3] Akalin Acar, Z. et al (2009) IEEE EMBC. [4] Korzeniewska, A et al (2008) HBM. [5] Neumaier and Schneider (2001). ACM TOMS. [6] Mullen,. T et al (2011). IEEE EMBC. [7] Mullen, T., et al (2010) http://sccn.ucsd.edu/wiki/SIFT